An Efficient E-learning and Internet Service Provision for Rural Areas Using High-Altitude Platforms during COVID-19 Pan-Demic

Sameer Alsharif , Rashid A. Saeed, and Yasser Albagory

Department of Computer Engineering, College of Computers and Information Technology, Taif University, P.O. Box 11099, Taif 21944, Saudi Arabia.

Summary
This paper proposes a new communication system for e-learning applications to mitigate the negative impacts of COVID-19 where the online massive demands impact the current commu-nications systems infrastructures and capabilities. The proposed system utilizes high-altitude platforms (HAPs) for fast and efficient connectivity provision to bridge the communication in-frastructure gap in the current pandemic. The system model is investigated, and its performance is analyzed using adaptive antenna arrays to achieve high quality and high transmission data rates at the student premises. In addition, the single beam and multibeam HAP radio coverage scenarios are examined using tapered uniform concentric circular arrays to achieve feasible communication link requirements.

Keywords:
COVID-19; e-learning; High-Altitude Platforms; Adaptive Arrays

1. Introduction

Different virus outbreaks seriously affect all life aspects and results in increasing infection and toll rates. COVID-19 has a very high infection rate between humans and spread to almost world territories [1-4]. Unfortunately, this virus is genetically variant and may last for a few years. Governments and health organizations recommend quarantine and increasing social distance to reduce the infection rate and mitigate the other consequences. The quarantine means that we should rely mainly on the online services that should be provided to the largest number of people worldwide, as possible. Many services such as e-commerce and e-learning services are used extensively and require a supporting communication network infrastructure as many employees, trainees, and students work home [5].

Despite the high demand on the Internet during this pandemic, some regions in a country suffer from the weak or even lack of communication network infrastructure that impedes the capability to support their population with e-services such as e-learning. Deploying terrestrial networks for these regions in a short time is impossible or requires very costly infrastructure. Therefore, governments can utilize satellite systems to pro-vide extensive coverage instead [6]. However, the considerable distance at which satel-lites operate, the special terrestrial transceivers and installation requirements are bar-riers to use such systems. Besides, satellite systems provide low data rates that may not suit the current package of the Internet services to meet people's requirements [7]. Another difficulty in Internet provision through satellites is the high rates of service provision, which is not suitable for the current economic breakdown. Therefore, a new communication system infrastructure should provide compatible high-speed Internet at low cost. Alternatively, high-altitude platforms provide superior comprehensive cov-erage and high-quality communication performance [8]. High-altitude platforms are airborne, balloons, airships, or unmanned aircraft that operate in the stratosphere and can provide coverage to an area of up to 1000 km diameter with a communication channel performance like satellite systems, but at very low relative altitudes.

Students in remote rural areas that suffer from the lack of communications services or inadequate cellular coverage with minimal Internet rates will not continue their distant e-learning. Therefore, flying airborne systems and moving them to such an in-accessible area provides instant wireless communication infrastructure that relieves [9]. In this paper, we consider the high-altitude platform to provide an efficient solution for the rapid establishment of the communication network to help students get e-learning services remotely [10]. The development of efficient antenna techniques at the high-altitude platform improves data rate provision to support internet services and the number of users.

1.2 Contribution

The main objective of this paper is to solve the problem of e-learing and Internet services provision for remote areas with undeveloped communication infrastructure. Therefore, the contributions of our work are to develop a novel end-to-end model for emergency and fast deployment electronic educational system, and to design a novel cross-layer between adaptive antenna, MAC layer and Application layer. We investigate the system mathematical and geometrical models and demonstrate the feasibility of the system.

Manuscript received March 5, 2024
Manuscript revised March 20, 2024
https://doi.org/10.22937/IJCSNS.2024.24.3.9

1.3 The Paper Organization

The paper is arranged as follows: Section 2 discusses the related cross layer opti-mization techniques for the current systems and HAPs. Section 2 discusses the current e-learning systems and their requirements, while Section 3 introduces the proposed HAP e-learning system model. In Section 4, we demonstrate the adaptive cellular e-learning HAP system using adaptive antenna arrays onboard HAP. Section 5 dis-cusses role of adaptive antenna arrays for coverage cells formation and adaptation. Section 6 shows the communication performance evaluation, and finally, Section 7 concludes the paper.

2. Related Works

Cross-Layer design is one of the most interested end-to-end system models that extensively used in the literature. It is the methodologies of manipulating the various parameters across the network layers from physical up to application layers. The proposed e-learning solution for Internet services provisioning over the HAP considers an end-to-end model that addresses all network layers. Therefore, we review the related works focus mainly on the cross-layer models in the literature, that addressing models associating adaptive antenna, MAC and application layers for multi-users. For instance, the author in [11] designed a sub-optimal power control for physical layer of uplink multiple antenna Non-orthogonal multiple access (NOMA) model to improve the overall data rates. For the video networks, the author developed an algorithm to reduce the overall video distortion and thus enhanced the signal-to-noise ratio (SNR). The results show that the proposed cross-layer method outperforms the physical layer by 1 db. The proposed method's complexity is tested and found that it is slightly better than that of the physical layer method [12]. The literature [13] proposed Cloud radio access network (C-RAN) to make strides range and vitality effectiveness of remote systems by relocating routinely disseminated BS capabilities into a centralized cloud baseband unit (BBU) pool. Besides, it proposed and explored a cross-layer asset assignment show for C-RAN to diminish the general framework control utilization within the BBU pool. It characterized such a problem as a mixed-integer nonlinear programming (MINLP). The accomplished reenactment proposed that the normal sparsity of the arrangement given by SP calculation is close to that gotten by the late proposed ravenous determination calculation, which has a higher computational complexity. The paper [14] proposed a cross-layer cooperative beamforming system with an ideal weight plan. For single-beam beamforming, closed-form ideal weights that maximize the signal-to-noise ratio (SNR) beneath a limitation of transmitting control are scientifically determined. The paper proposed two imperfect weight plans for multibeam beamforming to decide the weights that maximize ghostly productivity. The results validated the adequacy of the proposed two imperfect weight plans.

The author in [15] discussed a cross-layer design method for cross resource allocation and routing for physical (PHY) and MAC layers in multi-hop wireless backbone communications. They furnished the base stations (BSs) with smart antenna that can receive and transmit adaptive beam. A nonlinear optimization model is derived, which improves the throughput of the BSs under the PHY/MAC and routing assumptions. In addition, they utilized Dual disintegration to decouple such model into integrated sub-models that harmonized by the dual values at the various levels. The results verified the effectiveness of the proposed cross-layer model. The work in [16] suggested super-imposed Pilot (SiP) sequence-based channel estimation strategy for beamforming to help multi-antenna HAP arrive versatile radio communication frameworks. The proposed strategy misuses the earlier accessible data of users' spatial area, user's thickness, and a beamwidth of HAP directional receiving wire. Particularly, the author proposed area data supported and low power control SiP sequence-based Stage-wise Orthogonal Match Pursuit (StOMP) calculation to estimate channels, from single-antenna client terminals to beamforming, to help expansive scale multiple-antenna HAP [17]. A comparison of the proposed method with a notable reference procedure available within the literature is further discussed within the recreation.

The literature [18] proposed a user clustering and smart antenna for high altitude platform (HAP) massive MIMO models. The author exploited the fact that transmitted signal power mainly distillates on statistical-eigenmode (SE), and utilized it to achieve user clustering and model the outer-beamformer with minimized computational complexity. The paper also proposed a design for outer-beamformer by using the user minimized-dimensional SEs. The achieved simulation results illustrated the enhancement of the proposed beamforming method's performance in massive MIMO HAP models compared to the existing methods based on correlation channel matrix. The paper [19] highlighted the security at the physical layer on the general wireless networks security. Principally, networks establish a cross-layer scheduling method based on stochastic optimization theory to enhance all users' admission rates and ensure queue steadiness in all links. The method considered the restraints of physical-layer security (PLS) in various attacking strategies of conniving and non-conniving. The efficiency of the scheduling method is confirmed via simulation software. The results showed the influence of the number of antennae and attacking strategy on the scheduling approach.

In [20], it proposed a modern cross layer method that includes a concurrent shrewd smart antenna at the physical layer and arbitrary network coding at the network layer to enhance the overall network's performance. The smart antenna is utilized for dynamic transmitting power allocation to achieve power gain, while the random network coding is assumed to attain coding gain. The simulation results showed the effectiveness of the proposed method. The research in [21] investigated the long-term renewable smart energy disbursement reduction issue and expressed it as a stochastic optimization scheme. The paper developed nondeterministic polynomial hard (NP-hard) optimization problem as smart grid farm connectivity with minimal data rate. The proposed optimization problem is efficiently solved within accommodated computational complexity. Simulation results shown that the proposed successive approximation smart antenna (SABF) [22] scheme outperforms the zero-forcing smart antenna scheme (ZFBF) [23] in both smart grid disbursement and packet loss. The smart grid disbursement enhanced the packet loss under the proposed model by altering a control coefficient.

The researchers in [24] evaluated the performance of dynamic Minimum Variance Distortion-less Response (MVDR) and Least Squares (LS) smart antenna on the downlink (DL) channel from HAP to high mobility train. They assumed that the channel is flat fading and time-varying Rician (TVR). The dynamic MVDR smart antenna is more effective for the Rician fading channel. By developing the LS smart antenna, the results verified that the receiver can dynamically cope better than Rayleigh fading channel.

3. The Systems Requirements

The rapid advancement of distance learning (DL) technologies creates more chances to bailout educational systems in the shadow of such pandemic. Indeed, communication technologies thrive web-based distance learning and grant fair educational opportuni-ties for the largest population of students [25]. As a consequence of these innovations and other web development, universities and schools started to use distance learning platforms that are web-based to provide flexible education regardless of temporal and spatial differences [28]. Besides, the technical advancement in learning management systems (LMSs), such as Moodle, Blackboard, Claroline, ATutor, Desire2Learn (D2L), Dokeos, OLAT, eFront, etc. is the driving force for the modern implementation strate-gies. Moodle and Blackboard are the two most recognized web-based LMSs that are progressively used as platforms in general and higher educations. With different types of DL in concept, practice, and experience, these platforms are advancing rapidly to deliver a comfortable educational system [26].

Although internet penetration is expected to surpass 50 percent of the world pop-ulation by the end of 2020, more considerable broadband penetration and telecommu-nications services are needed for impoverished people and remote rural areas. Due to adequate infrastructures, distance education and e-exam can be affordable properly in metropolitans and cities. However, the currently available broadband access technolo-gies still not mature enough in remote regions. Qualified rural broadband applications with minimal cost are required to increase internet accessibility. Such objective can be achieved by the wide spectrum of accessible and scalable wireless technologies [27]. Therefore, traditional distance learning system essentially requires a highly secured wireless communication platform with affordable prices. Such a platform holds some criteria such as two-way communications, real-time video streaming, file sharing, and deliberations. Broadband access is efficient, cost-effective, and fast-deployment tech-nologies to improve accessibility. Economic and technological considerations derive the critical challenges of delivering broadband networks in remote areas [29]. For instance, the configuration of fiber optic backhauls connectivity or 4G deployment in the rural counties remain an expensive option. Networks operators should develop a new broadband wireless access technology to overcome the said challenges. The new tech-nology possesses the following properties, 1-visible enough to operate with low power, 2- with low provisioning cost, 3- it is a rigid type of climate, and 4- fading channels technology. Although the researchers extensively investigated this subject, such chal-lenges still need to be considered for e-learning in remote territories. These challenges range from the physical to network layers and include quality of services for real-time, delay-sensitive applications, offline storage spaces, recording, and data retrieval.

Wireless high-altitude platform (HAP) communication is an alternative compro-mising solution to supply distance learning [30]. Networks operators can utilize HAP systems to provide fixed broadband connectivity for end remote area users, including mountainous, coastal, and desert areas. HAP needs a lower venture and operation costs to certain extents and provides high quality of services and enough capacity for e-learning. In pandemic situations like COVID-19, HAP can be rapidly deployed for DL because it allows for the establishment of services with minimal ground network in-frastructure. HAP also can be reallocated to different locations easily with minimum cost

4. Adaptive E-learning Provision from HAPS

4.1 System Architecture

Figure 1 shows e-learning services provision from HAP by adaptive antenna arrays system onboard HAP fed by the coverage information from the university site's ground station. The beamforming information is defined according to the registered report of students on the university e-learning database, such as home locations, academic schedule, the number of students existing in a common remote region, the minimum services bit rate, etc. This information is extracted at the HAP beamformer input to di-rect suitable beams for students' locations. The HAP acts as a repeater in this case and can be considered as a fixed "stratospheric satellite" [32]. The beamforming can be cre-ated by many suitable planner antenna structures, such as two-dimensional arrays or concentric arrays. This paper considers the concentric arrays due to their performance superiority and azimuth-independent beam generation property. The taper profile function feeds the array to improve the sidelobe performance and reduce the co-channel interference if frequency-reuse is applied.

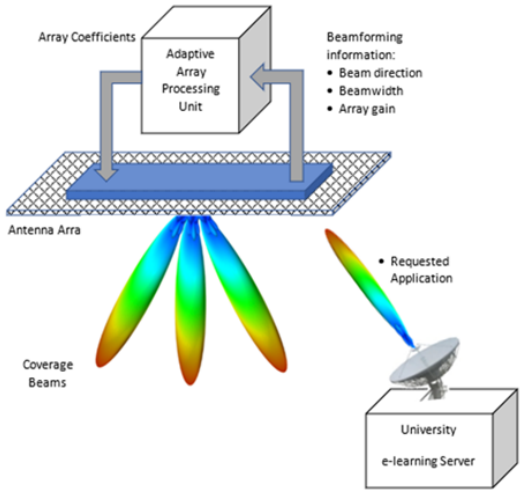

Figure 1. Adaptive antenna array HAP system for e-learning services provision.

Figure 2 shows the distribution for HAP coverage cells. The system splits the coverage into different area coverage (residential area) and antenna spot beams within the residential area. We assume that we have N residentials areas, M spot beams and P applications and services within each beam. The proposed model for managing appli-cations is based on socket and port numbers, where the network administrator identi-fies the privilege for each application. The beam data rate is Cm, while the network operation center, NOC, data rate is CT. We distribute the beams and the associated data rates based on users' activities and application priorities.

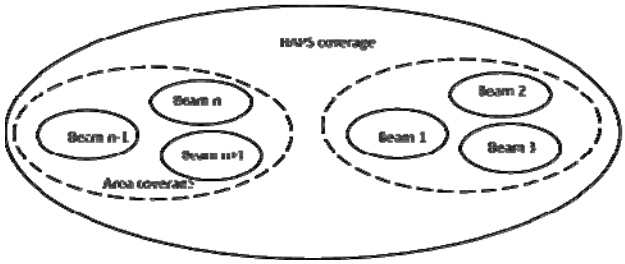

Figure 2. the physical distribution for HAPS signal

The system starts with allocating total data rate, CT, at NOC, applying policies, limitations, and calculates the required antenna array feeding currents to form a cov-erage beam. Then, it receives the requester's order and verifies that the beam covers it. If the requester is out of the beam coverage, the system forms a new beam and allocates resources to the MAC. Then, calculate the data rate in the formed beam to allocate more resources in such beam. Once the beam array is created with the corresponding data rate and the resources are assigned, the system checks that the requested application is open. If the application is open, the system applies for limitation roles, receives more appli-cations, and checks their types. It gives the best-allowed resources for the application within the schedule, and it is ready to welcome new requests. But if the application is not in the plan, it verifies that the application is permitted to give the best effort re-sources. Otherwise, it should block the application. If the application originally is not open, the program calls the application layer for data rate adaptation. The flowchart of such planning is shown in Figure 3.

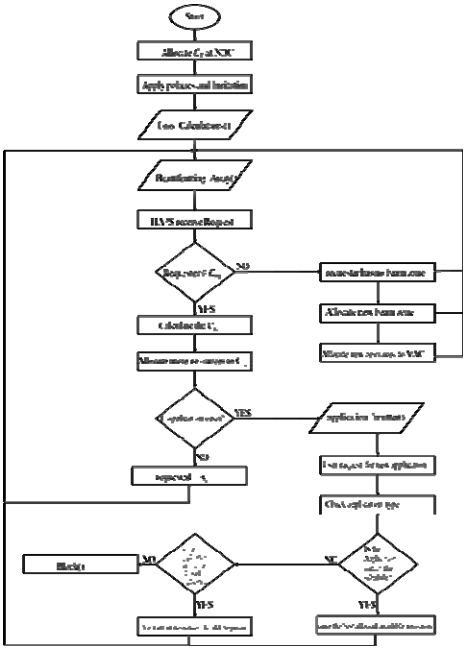

Figure 3. an algorithm of resources distribution in HAPS.

4.2 System Adaptation Parameters

This section demonstrates and discusses the system adaptation parameters for HAP e-learning services. These parameters include the operation on both the applica-tion and physical layers to control the data rates of different e-learning applications and the overall cell data rate. Equation (1) shows the total NOC link capacity:

$$C_T = \sum_{n=1}^{N} \sum_{m=1}^{M} \sum_{p=0}^{P} C_m(n,p) \quad (1)$$

Where C_m is calculated based on the cross-layer model for physical and application layer data rates for each beam in a specific area. Simply, C_m can be controlled as follows:

$$C_m(n,p) = \emptyset(R_m, A_m) \quad (2)$$

where R_m and A_m are the rate adaptation parameters of physical and application layers, respectively. In e-learning communication system, students need to access a limited number of applications which can be classified into three main categories: e-learning platforms such as Blackboard, video streams, and general web access. The data rate for each type depends on the number of students in each area where the one with a large student population is expected to get a fair share from total data rate, C_T. To equitably distribute C_T, we use the same level source utilization approach to manage resources proportionally with the student population in each coverage area.

Proportional utilization coefficient, K_u, is the result of a division of student population in a given area, S_t, by the total number of students that included by coverage, S_{total}, i.e.:

$$K_u = \frac{S_t}{S_{total}} \quad (3)$$

Then, the total data rate designated for the i area with multiple beams, B_i, is given as follows:

$$B_i = \sum_{m=1}^{M} \sum_{p=1}^{P} C_m(i,p) \quad (4)$$

Which can also be expressed as:

$$B_t = K_u C_T \quad (5)$$

The NOC can dedicate η of the data rate in the i[th] area to e-learning platform, EL_i, because of students' need to classes attending, assignments uploading, and exams taking. On the other hand, students might need to watch some supplementary tutorials via different video streaming platforms, VS_i, which is ζ of the data rate and may be smaller than η to avoid abusing data consumption. Finally, δ of data rate in a specific area is devoted to web browsing, WB_i, to help students search or find written tutorials. Mathematically, equations (6) to (8) depict such distributions as follows:

$$EL_t = \eta\ B_t \quad (6)$$

$$VS_t = \zeta\ \ B_t \quad (7)$$

And

$$WB_t = \delta\ B_t \quad (8)$$

To find data rate for each student in the same area for a specific service such as e-learning, we divide EL_t by the number of students in such area as follows:

$$EL_{S_t} = \frac{EL_t}{S_t} \quad (9)$$

Eventually, we express the application layer data rate adaptation parameter for the i[th] beam, A_m, as follows:

$$A_m = \frac{EL_t + VS_t + WB_t}{M} \quad (10)$$

To compare such a scheme to the typical e-learning services with the corresponding data rates, table 1 lists some of them.

Table 1. Typical standard data rates for some of the e-learning services

E-learning services	Data rate
Standard definition (SD) video	2 Mbps
High definition (HD) video	5 Mbps
E-mail and web browsing	500 kbps
Downloading e-books	2 Mbps
Online exam and assessment	100 kbps

The other physical layer adaptation factor for C_m, R_m, represents the capability to control the mth cell gross data rate that should be balanced according to the number of students in each cell. Therefore, we can consider R_m as the cell radius which should be controlled to accommodate a suitable number of students in the cell which effectively controls the required gross data rate for that cell, i.e. C_m. The next section presents the implementation of such adaptation, harnessing adaptive antenna arrays onboard HAP.

5. HAP Cell Coverage Adaptation Using Onboard Antenna Arrays

This section demonstrates the physical coverage cells formation and adaptation. First, it illustrates the coverage area, cell geometry and shows the controlling parameters. Second, it shows how to link the coverage cell area with the HAP antenna array system to achieve the required adaptation process.

5.1 HAP Coverage Cell Formation and Control

We can address the problem of delivering local e-learning services by incorporating the e-learning management system into the communication facility to bridge the information gap in distant or isolated regions. Consider the HAP station located at an altitude of h km in the stratosphere, as shown in Figure 4. The maximum coverage diameter can be obtained by:

$$\rho_o = r\cos^{-1}\left(\frac{r}{r+h}\right) \quad (11)$$

Where, r is the earth radius.

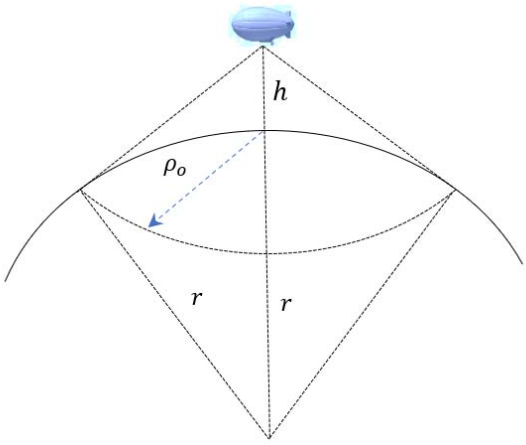

Figure 4. Maximum HAP coverage area and radius.

The maximum diameter of HAP coverage can extend to about 1000 km for a HAP located at the height of 20 km. However, due to shadowing effects, the coverage diameter is lowered practically to a few hundreds of kilometers. The coverage zone may be much less-wide for local regions corresponding to the main university campus and could extend to 300 kilometers according to the district distribution. Therefore, such a system delivers interactive e-learning services to students in remote locations which suffer from low or limited connectivity. The controlling parameters for the system design can be defined as follows:

- Student density in remote areas,
- Minimum bit rate requirements for each student,
- Communication channel capacity, C_m
- HAP altitude, h

Some beaming techniques such as directional spot-beam antennas or antenna arrays provide service beam from HAP. The spot-beam directional antennas are more suitable for fixed service applications where the coverage area per beam is constant. On the other hand, adaptive antenna arrays adapt to system variant conditions such as university schedule, student density, services bit rates, etc. The beam shape and gain vary with these parameters. The system can harness several antenna array structures such as two-dimensional arrays and concentric circular arrays (CCA), which are used in this work for HAP communications.

Figure 5 shows the concentric arrays with unifo rm elements separation at the half-wavelength dista nce between elements in the same ring and betwee n concentric rings. The taper profile is applied cent rically on the rings where the highest feeding ampl itude feeds the innermost ring elements. The phase responses of the elements are adjusted to direct th e mainlobe toward the desired region. Also, the be am width can be adjusted by either controlling the

taper profile or the number of utilized rings in the array [33-38].

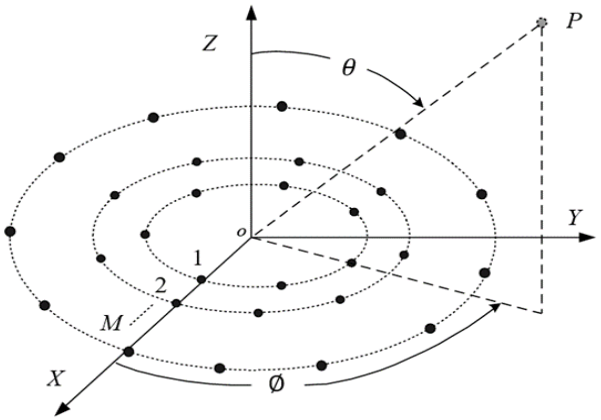

Figure 5. Concentric circular antenna arrays

Therefore, the array power gain can be written as follows:

$$G_t(\theta,\emptyset) = |\boldsymbol{W}(\theta_o,\emptyset_o)^H \boldsymbol{S_{CA}}(\theta,\emptyset)|^2 \quad (12)$$

Where, $\boldsymbol{W}(\theta_o,\emptyset_o)$ is the weighting vector of the array, $\boldsymbol{S_{CA}}(\theta,\emptyset)$ is the array steering vector [33], and H is the Hermitian operator. If the number of elements in the k[th] ring in the concentric array is L_k, and K rings form the array; the weighting vector is given as follows:

$$\boldsymbol{W}(\theta_o,\emptyset_o) = \boldsymbol{\Gamma} \odot \boldsymbol{S_{CA}}(\theta_o,\emptyset_o) \quad (13)$$

Where $\boldsymbol{\Gamma}$ is the subarrays weighting coefficients, $\odot$ is the Hadamard product, and $\boldsymbol{S_{CA}}(\theta_o,\emptyset_o)$ is the array steering vector which corresponds to the main-lobe direction.

Finally, $\boldsymbol{\Gamma}$ is expressed as follows:

$$\boldsymbol{\Gamma} = \begin{bmatrix} \boldsymbol{\alpha_1} \\ \boldsymbol{\alpha_2} \\ \vdots \\ \boldsymbol{\alpha_m} \\ \vdots \\ \boldsymbol{\alpha_M} \end{bmatrix} \quad (14)$$

here $\boldsymbol{\alpha_k}$ is a colon sub-vector of L_k elements of the same amplitude coefficient value α_m.

The k^{th} subarray amplitude coefficient α_k is proposed as follows:

$$\alpha_k = \left(\cos\left(\frac{(k-1)\pi}{2K}\right)\right)^{2.3}, k = 1,2,\dots,K \quad (15)$$

Generally, as shown in Figure 6, the mth service beam from HAP can cover an area, a_m, that is given by:

$$a_m = \pi R_m^2 \cos(\theta_m) \quad (16)$$

where, R_m is the footprint half-major axis in θ_m direction and is given by:

$$R_m = h\left(\tan(\theta_m) - \tan\left(\theta_m - 0.5\, B^{\theta}\right)\right) \quad (17)$$

and B^{θ} is the beamwidth in the θ_m direction. Therefore, the cell area can be related directly to the beamwidth and direction as follows:

$$a_m = \pi h^2 \left(\tan(\theta_m) - \tan\left(\theta_m - 0.5\, B^{\theta}\right)\right)^2 \cos(\theta_m) \quad (18)$$

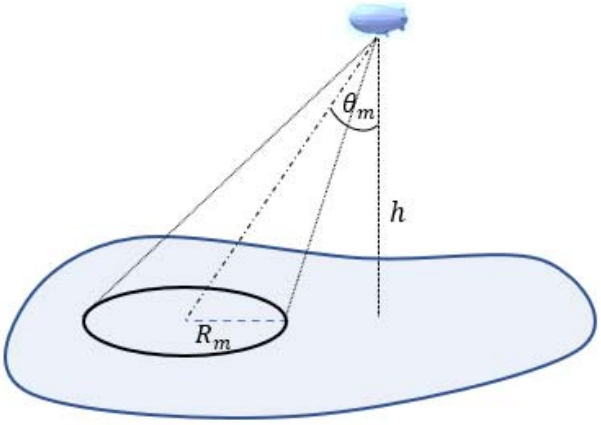

Figure 6. Spotbeam coverage from HAP

Figure 7 displays the cell area's variation with the beam direction at different beamwidth values. As shown in this figure, for beam directions up to 40° especially for small beamwidths, the beamwidth mainly controls the cell area where the effect of beam direction is negligible. Increasing beam direction beyond this limit results in a rapid increase in the cell area because of projection on the earth's surface, where the cells become more elliptical.

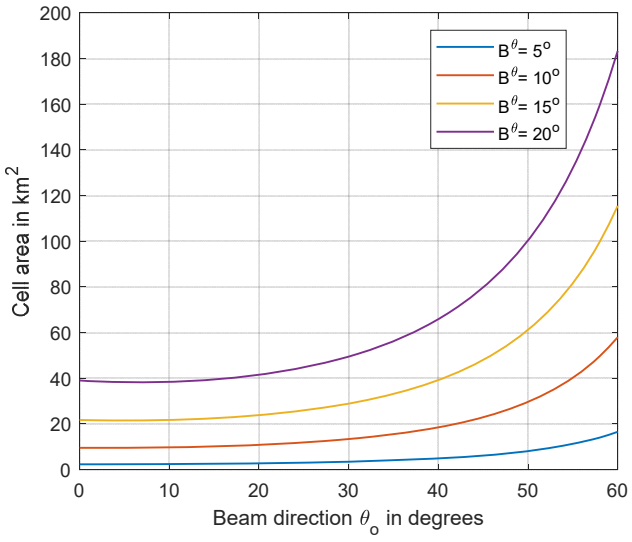

Figure 7. Variation of the coverage area with beam direction at different beamwidths.

The system links the total number of students located in a cell with the cell area from the following relation:

$$S_m = D_s a_m \tag{19}$$

Where, D_s is the student density in the remote or isolated area. On the other hand, we can design the coverage beam from the following relation:

$$a_m = \frac{S_m}{D_s} \tag{20}$$

Therefore, we can design the required coverage beam for a specific number of students and density for this area.

5.2 Communication link performance at the student premises

The signal level and probability of error at the student premises should be acceptable to achieve a specific communication link performance. The received signal power level at the student e-learning receiver input, P_s, can be written as:

$$P_s = P_t G_s G_t(\theta, \emptyset) \left(\frac{\lambda}{4\pi d_s}\right)^2 \frac{1}{\xi} \tag{21}$$

Where,
P_t is the HAP transmitted power,
G_s is the receiver antenna power gain,
$G_t(\theta, \emptyset)$ is the HAP transmitting antenna gain,
λ is the signal wavelength,
d_s is the slant distance between the HAP and the student receiver,
ξ is an excess attenuation due to atmospheric losses, shadowing, fading, and extra margin for the communication link.

Assuming QPSK modulation scheme, the probability of error at the student receiver is given by [39]:

$$p_e = \frac{1}{2} erfc\left(\sqrt{\frac{P_s}{N_0 B_s}}\right) \tag{22}$$

where, N_o is the noise power spectral density, $erfc$ is the complementary error function, and B_s is the student accessible bit rate. Therefore, the signal strength and the communication link quality depend mainly on the received signal power from HAP and the required bit rate. Larger bit rates require more substantial received power to maintain the probability of error within an acceptable range. Therefore, the antenna gain at HAP plays an essential role in achieving the required e-learning services quality for students in remote areas. We can manage the beam downlink capacity from HAP toward a specific area by adapting students' schedules to deliver the highest possible data rate for them. For example, suppose the maximum beam downlink speed of the overall e-learning channel is 1 Gbps, and each student can be assigned 2 Mbps. In that case, the total number of simultaneously served students is less than or equal to 500 students. The service beam from HAP can be split into multibeam when the number of simultaneously served students is less than the beam capacity, where the coverage footprint can be extended to cover other remote regions. In the next section, we demonstrate the adaptive array structure at HAP that achieve the objective of adapting both the beam power gain and coverage area according to the remote area location and number of students.

5. Numerical Results and Discussions

This experiment validates and tests the system's capability to provide communication links with feasible performance and requirements. The system simulation parameters are listed in Table (2), as shown below, including physical and applications settings. The onboard antenna array structure includes the number of elements and their distributions, interelement separation, operating frequency, bandwidth, HAP height, application data rates, percentages, etc. The test is in two scenarios: the formation of single beam coverage and the capability to provide

multibeam coverage based on the same weights or coefficients.

Table 2. Simulation parameters and their values

Simulation parameter	value
Antenna elements type	Isotropic radiators
Number of rings, $\boldsymbol{K}$	10 rings
Innermost ring size	5 elements
Interelement spacing	λ/2
Inter-ring spacing	λ/2
Number of elements in each ring, $\boldsymbol{L_K}$	5, 11, 17, 23, 29, 35, 41, 47, 53, and 59
Outermost ring size	59 elements
HAP altitude	20 km
Total HAP coverage zone	*80 km X 80 km*
Main lobe direction for single beam	(50°,45°)
Main lobe directions for multi beams	(50°,45°), (45°,135°), and (45°,300°)
Beam carrier frequency	5 GHz
Channel bandwidth	20 MHz
Beam transmitted power	30 Watts
Maximum free space loss	142 dB
Noise power spectral density, $\boldsymbol{N_o}$ in dBm/Hz	-174 dBm/Hz
Minimum received signal power in dBm	-70 dBm
Percentage of e-learning data rate, η	50%
Percentage of video streaming data rate, ζ	20%
Percentage of web browsing data rate, δ	30%

6.1 Single Beam Scenario

In this scenario, the concentric rings are weighted as shown in Figure 8, which are normalized. The maximum weight is assigned to the innermost ring, while the outermost ring has the lowest weight value. This tapered profile is proposed mainly for sidelobe reduction, which is essential for reducing the unwanted radiation towards other co-channel beams.

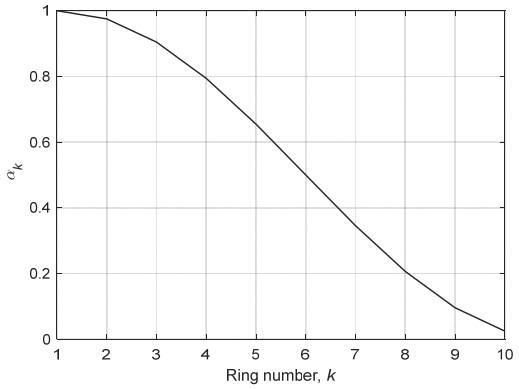

Figure 8. Weighting coefficients for the concentric ring array to form single coverage beam.

We examined the radio coverage from HAP for a single beam generated towards an arbitrary direction of (50°, 45°). The center of the cell is located at approximately 35 km from the sub-HAP point, while the end-of-coverage extends to about 56 km. The footprint shown in Figure 9 represents the array power gain for a concentric array of 10 rings with 5 antenna elements in the innermost ring. The antenna elements are considered isotropic radiators, and the peak power gain of the array is 40 dB using the weighting profile in Figure 8. Figure 10 shows the free-space path loss investigation where it ranges from -132.5 at the sub-HAP point to -142 dB at the end-of-coverage, where the maximum line-of-sight distance at the end-of-coverage is 60 km. In this case, the coverage area is considered a square of 80 km side length, suitable for local university coverage. The free-space-loss affects the student premises' received signal level and should be considered in the link budget calculations. Also, for remote regions that are far from the university campus, the coverage can be secured by locating the HAP at a suitable location that can be directly seen from the university sight. Consequently, higher gain directional backhaul antennas are required at the university site to boost signals to/from HAP.

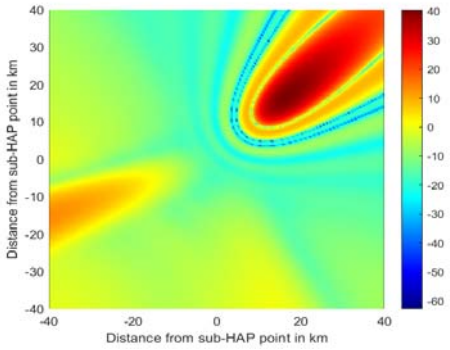

Figure 9. HAP antennae gain in dB and cell footprint.

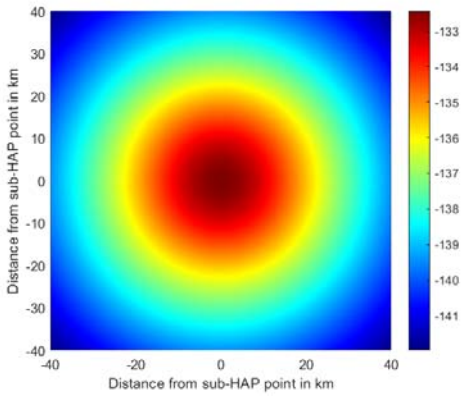

Figure 10. Free-space loss in dB that affect the transmitted signal from HAP located at 20 km high and covering a square area of $80km \times 80km$.

If we consider a 30 Watt of transmitted HAP beam power with a 10 dB extra attenuation margin, then, the resulting received power in dBm over the beam coverage region is shown in Figure 11, where the main-lobe spot is shown in dark red has power levels of more than -50 dBm.

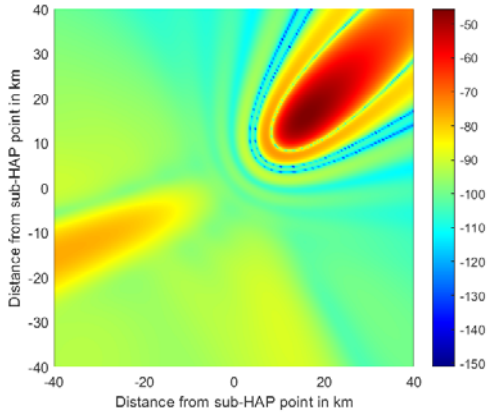

Figure 11. Received signal strength in dBm and footprint.

For a channel bandwidth of 20 MHz, the probability of error for QPSK modulated digital signals is shown in Figure 12 for the coverage region where the brown ellipse represents the area that has an error of less than 10^{-13} which fits the required link quality and assures stable transmission for most communication services.

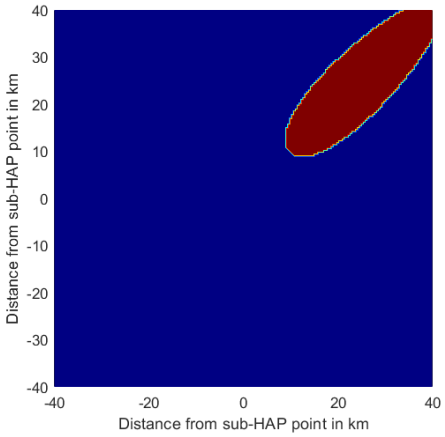

Figure 12. Probability of error footprint for the single beam coverage scenario from HAP. Brown region has $p_e < 10^{-13}$.

6.2 Multi Beam Scenario

In this scenario, the antenna array beamforming system is examined to form multibeams using the same elements and weighting function for feeding these elements as shown in Figure 13 to form three simultaneous beams with the directions listed in Table 2.

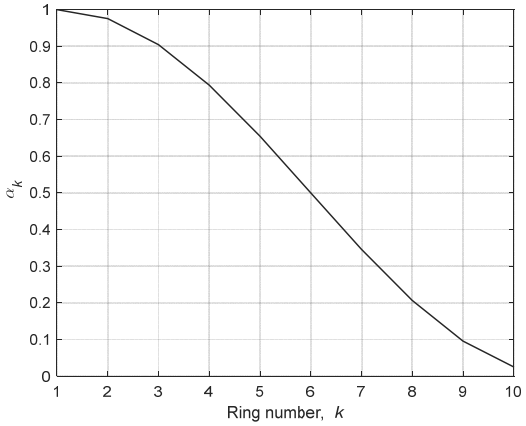

Figure 13. Weighting coefficients for the concentric ring array to form multibeam coverage.

The weights in this figure are very similar to the single beam scenario. They can be considered the sum of three individual weighting vectors corresponding to the individual beams in the multibeam structure. Generally, for M spotbeams, the array weighting function can be written as follows:

$$\boldsymbol{W_M} = \sum_{m=1}^{M} \boldsymbol{W}(\theta_{om}, \emptyset_{om}) \tag{23}$$

For example, as shown in Figure 13, three arbitrary beams directed at $(50°, 45°)$, $(45°, 135°)$, and $(45°, 300°)$ can be formed using Eq. (23). The system can control the HAP transmitted power to provide higher values

of received signal powers at the student premises, especially at the end-of-coverage regions. The red colored represents the regions with acceptable levels of received power that are almost higher than -70 dBm. On the other hand, if the student receiver is equipped with directional antennas, the received power can be further improved.

The received signal quality is depicted in Figure 14 for the above multibeam scenario, where the brown regions with a probability of error less than 10^{-13} to meet the required service quality. A 20 MHz channel capacity at 5 GHz is approximately 380 Mbps which roughly can serve about 190 students simultaneously over the covered spot areas with 2 Mbps delivery for each student. Several channels or wider channel bandwidths along with suitable multiple access schemes can be utilized using the 5G spectrum at higher frequencies such as 6 GHz with bandwidths more than 100 MHz to provide more than 1 Gbps data rates that can accommodate a larger number of students in the remote areas.

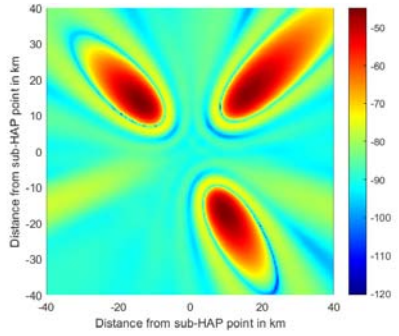

Figure 14. Beam received signal strength in dBm and footprint for multibeam coverage scenario from HAP.

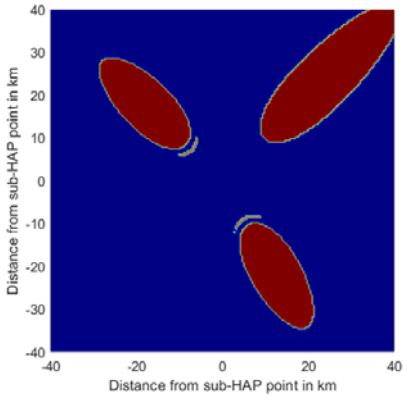

Figure 15. Probability of error footprint for the multibeam coverage scenario from HAP. Brown regions has $p_e < 10^{-13}$.

7. Conclusion

This paper proposed a novel end-to-end communication network for robust, fast deployment, and efficient e-learning services for sparse areas using high-altitude platforms (HAPs) system. The network design is examined and investigated, where we classified the data from the server into three categories, including different services, including e-learning activities, video streaming, and web browsing. The highest priorities are devoted to online classes and discussion applications, while the other applications are assigned lower priorities. On the other hand, adaptive antenna arrays are proposed for coverage beam adaptation and distribution for efficient resource management and improving the overall throughput that enters the HAP link. These beams are manipulated and dynamically adapted using MAC and application layers parameters such as the services data rates. The proposed model is simulated. The system performance is analyzed where the results showed that using an adaptive antenna array can achieve high quality and high rate of transmission data at the student premises with feasible requirements for both single beam and multibeam coverage scenarios.

Acknowledgments

The authors would like to thank Taif University for supporting this work under project number (1-441-82).

References

[1] https://www.cdc.gov/coronavirus/2019-nCoV/index.html. Last visit was in March 2, 2021
[2] https://www.worldometers.info/coronavirus. Last visit was in March 2, 2021
[3] https://www.cdc.gov/globalhealth/countries/saudi_arabia/default.htm. Last visit was in March 2, 2021
[4] https://www.gsma.com/coverage/. Last visit 3 March 2, 2021
[5] Arum, S. C.; Grace, D.; and Mitchell, P. D. A review of wireless communication using high-altitude platforms for extended coverage and capacity. Computer Communications 2020, Volume 157, Pages 232-256, ISSN 0140-3664, https://doi.org/10.1016/j.comcom.2020.04.020.
[6] Mohammed, A.; and Yang, Z.; Broadband Communications and Applications from High Altitude Platforms. International Journal of Recent Trends in Engineering 2009, Vol 1, No. 3, May 2009.
[7] Karapantazis, S.; and Pavlidou, F. Broadband communications via high-altitude platforms: a survey. IEEE Communications Surveys & Tutorials 2005, vol. 7, pp. 2-31.
[8] Oodo, M.; Miura, R.; Hase, Y.; Inaba, T.; Sakamoto, T.; and Suzuki, M. Measurement results of digital beamforming array antenna onboard stratospheric platform in the band 31/28 GHz. Proceeding of 5th International Symposium on Wireless Personal Multimedia Communications 2002, Honolulu, Hawaii, October 2002.
[9] Xu, Z.; Zakharov, Y.; and White, G.; Vertical antenna array and spectral reuse for ring-shaped cellular coverage from High Altitude Platform. Loughbourgh Antennas and Propagation Conference (LAPC 2006), November 2005.
[10] Isernia, T.; Ares Pena, F. J.; Bucci, O. M.; D'Urso, M. ; Gomez, J. F.; and Rodriguez, J. A.; A hybrid approach for the optimal synthesis of pencil beams through array antennas. IEEE Transactions Antennas and Propagation 2004, Vol. 52, No.11,pp. 2912–2918.
[11] Tseng, S.M.; Chen, Y.F.; and Fang, H.H. Cross PHY/APP Layer User Grouping and Power Allocation for Uplink Multiantenna NOMA Video Communication Systems. IEEE Systems Journal 2020, Volume:14, Issue: 3.
[12] Ibrahim, A.; Alfa, A. S. Radio Resource Allocation and User Admission Control in HAPs. Optimization Methods for User Admissions and Radio Resource Allocation for Multicasting over High Altitude Platforms, Book Chapter, River Publishers, 2018.

[13] Tang, J; Tay, W. P, ; Quek, T. Q. S. Cross-Layer Resource Allocation With Elastic Service Scaling in Cloud Radio Access Network. IEEE Transactions on Wireless Communications 2005, Volume: 14, Issue: 9.
[14] Xinghua, S; Xiaoxiang, W.; Weiling, W. Cross-layer Resource Allocation for the Downlink of SDMA Systems. 2007 International Workshop on Cross Layer Design, 2007.
[15] Zakia, I.; Tjondronegoro, S.; Iskandar; Kurniawan, A. Performance comparisons of adaptive MVDR and received LS beam-forming on the downlink time varying channel of HAP system. 2013 19th Asia-Pacific Conference on Communications (APCC), 2013
[16] Kim, S.-J., Wang, X., & Madihian, M. Cross-Layer Design of Wireless Multihop Backhaul Networks With Multiantenna Beamforming. IEEE Transactions on Mobile Computing 2007, 6(11), 1259–1269. doi:10.1109/tmc.2007.1052.
[17] Nawaz, S. J.; Mansoor, B.; Sharma, S. K.; Gulfam, S. M. and Patwary, M. N. Location-Aware and Superimposed-Pilot Based Channel Estimation of Sparse HAP Radio Communication Channels. 2017 IEEE 85th Vehicular Technology Conference (VTC Spring), Sydney, NSW, Australia, 2017, pp. 1-7, doi: 10.1109/VTCSpring.2017.8108354.
[18] Lian, Z., Jiang, L., He, C., & He, D. User Grouping and Beamforming for HAP Massive MIMO Systems Based on Statisti-cal-Eigenmode. IEEE Wireless Communications Letters 2019, 1–1. doi:10.1109/lwc.2019.2902140
[19] Lun Dong, Petropulu, A. P., & Poor, H. V. Weighted Cross-Layer Cooperative Beamforming for Wireless Networks. IEEE Transactions on Signal Processing 2009, 57(8), 3240–3252. doi:10.1109/tsp.2009.2020048.
[20] Li, B., Li, H., & Zurada, J. M. Cross-Layer Design of Joint Beamforming and Random Network Coding in Wireless Multicast Networks. IEEE Communications Letters 2014, 18(12), 2173–2176. doi:10.1109/lcomm.2014.2352297.
[21] Jun Wang, Pengfei Huang, Xudong Wang, & Yang Yang. Cross-layer scheduling for physical layer secrecy and queue stability in a multi-user system. 2013 IEEE Global Communications Conference (GLOBECOM). doi:10.1109/glocomw.2013.6855662.
[22] Yu, J.; Cai, Y.; Ma, Y.; Zhang,D.; & Xu, Y. A cross-layer design of packet scheduling and resource allocation for multiuser MIMO-OFDM systems. 2007 6th International Conference on Information, Communications & Signal Processing. doi:10.1109/icics.2007.4449629.
[23] Huang, W. L., Letaief, K. B., & Zhang, Y. J. Cross-Layer Multi-Packet Reception Based Medium Access Control and Resource Allocation for Space-Time Coded MIMO/OFDM. IEEE Transactions on Wireless Communications 2008, 7(9), 3372–3384. doi:10.1109/twc.2008.060327.
[24] Ibrahim, A.; and Alfa, A. S. Multicasting in a Single HAP System: System Model and Mathematical Formulation"", Optimi-zation Methods for User Admissions and Radio Resource Allocation for Multicasting over High Altitude Platforms, 2018.
[25] Dong, Y; Hossain, M. J.; Cheng, J; Leung, V. C. M. Dynamic Cross-Layer Beamforming in Hybrid Powered Communication Systems With Harvest-Use-Trade Strategy. IEEE Transactions on Wireless Communications 2017, Volume: 16, Issue: 12.
[26] Yu-Dong Yao, Syed, M., & Jin Yu. Utilizing beamforming for random access - a cross-layer paradigm. IEEE 60th Vehicular Technology Conference, 2004. VTC2004-Fall. 2004. doi:10.1109/vetecf.2004.1405084
[27] Choi, J. P.; & Joo, C. Cross-layer optimization for satellite-terrestrial heterogeneous networks. 2014 International Conference on Computing, Networking and Communications (ICNC). doi:10.1109/iccnc.2014.6785345.
[28] Xiao, K.; Li, C.; & Zhao, J. LSTM Based Multiple Beamforming for 5G HAPS IoT Networks. 2019 15th International Wireless Communications & Mobile Computing Conference (IWCMC). doi:10.1109/iwcmc.2019.8766663.
[29] Luo, X.; Xu, J.; Zou, Y., Gong, S.; Gao, L.; & Niyato, D. Collaborative Relay Beamforming with Direct Links in Wireless Powered Communications. 2019 IEEE Wireless Communications and Networking Conference (WCNC). doi:10.1109/wcnc.2019.8886084.
[30] Sudheesh, P. G.; Mozaffari, M.; Magarini, M.; Saad, W.; & Muthuchidambaranathan, P. Sum-Rate Analysis for High Altitude Platform (HAP) Drones With Tethered Balloon Relay. IEEE Communications Letters 2017, 22(6), 1240–1243. doi:10.1109/lcomm.2017.2785847.
[31] Arum, S.C.; Grace, D.; Mitchell, P.D.; Zakaria, M.D.; Morozs, N. Energy Management of Solar-Powered Aircraft-Based High Altitude Platform for Wireless Communications. Electronics 2020, 9, 179. https://doi.org/10.3390/electronics9010179.
[32] G. White, E. Falletti, Z. Xu, D. Borio, F. Sellone, Y. Zakharov, L. Lo Presti, F. Daneshgaran "Report on adaptive beamforming algorithms for advanced antenna types for aerial platform and ground terminals", CAPANINA Project, Deliverable No. D17, 31st Jan 2006.
[33] Dessouky, M.; Sharshar, H.; and Albagory, Y. Efficient sidelobe reduction technique for small-sized concentric circular arrays. Prog. Electromagn. Res. 2006, vol. 65.
[34] Choi, Y.-S.; Park, J.-S.; Lee, W.-S. Beam-Reconfigurable Multi-Antenna System with Beam-Combining Technology for UAV-to-Everything Communications. Electronics 2020, 9, 980. https://doi.org/10.3390/electronics9060980.
[35] Dessouky, M.; Sharshar, H.; and Albagory, Y. An approach for Dolph-Chebyshev uniform concentric circular arrays. J. Elec-tromagn. Waves Appl. 2007, vol. 21, no. 6.
[36] Dessouky, M.; Sharshar, H.; and Albagory, An Approach for Low Sidelobe Beamforming in Uniform Concentric Circular Arrays. Wireless Personal Communications 2007, vol. 43, no. 4, pp. 1363-1368, 2007, Springer.
[37] Nofal, M.; Aljahdali, S.; and Albagory, Y. Tapered beamforming for concentric ring arrays. AEU - Int. J. Electron. Commun. 2013, vol. 67, no. 1, pp. 58–63.
[38] Albagory, Y. An Efficient Conformal Stacked Antenna Array Design and 3D-Beamforming for UAV and Space Vehicle Communications. Sensors 2021, 21, 1362. https://doi.org/10.3390/s21041362
[39] Digital Communications, John Proakis, Massoud Salehi, McGraw-Hill Education, Nov 6, 2007.

.